Working Paper

Glaciers as Indicators of Climatic Change – Background and Tools for Modelling

Johannes Oerlemans

WP-93-32
June 1993

IIASA International Institute for Applied Systems Analysis □ A-2361 Laxenburg □ Austria
Telephone: +43 2236 715210 □ Telex: 079 137 iiasa a □ Telefax: +43 2236 71313

Glaciers as Indicators of Climatic Change – Background and Tools for Modelling

Johannes Oerlemans

WP-93-32
June 1993

International Institute for Applied Systems Analysis □ A-2361 Laxenburg □ Austria
Telephone: +43 2236 715210 □ Telex: 079 137 iiasa a □ Telefax: +43 2236 71313

Abstract

Glaciers may be used as indicators of climatic change. This paper presents data from six glaciers with records of glacier length greater than 200 years. All show a strong retreat since 1850. The paper discusses past work to model these glaciers based on climatological time series from nearby station. Studies performed until now have not produced good results and have only partially described the retreats of the past 100 years.

A new, two-step modelling approach is presented here. The first component relates climate conditions to glacier mass balance followed by a second which calculates ice flow as a response to imposed mass balance.

The mass balance approach uses an energy balance on the glacier surface, explicitly accounting for turbulent fluxes in the atmospheric boundary layer above the glacier surface and for the changes in albedo in the modelling of radiation. Meteorological data needed to run the mass balance module are temperature and humidity, cloudiness, and precipitation.

A one-dimensional flow model based on equations of the continuity and motion is used to compute the dynamics of a glacier along the centerline down the surface slope. It takes into account varying lateral geometry, sliding and deformation of the glacier and changes in ice thickness.

The coupled, two-component model system is solved using an explicit scheme for time integration. Various numerical techniques to improve computational efficiency are discussed.

Preliminary results of this approach have been promising and will be discussed by a follow-up paper.

Glaciers as Indicators of Climatic Change - background and tools for modelling

IIASA Working Paper

Johannes Oerlemans#

on leave from the Institute for Marine and Atmospheric Research Utrecht, Utrecht University, with support from the Netherlands Organization for Scientific Research

Contents

1. Introduction - some definitions and concepts

When continuing for many years, accumulation of snow and ice will lead to the formation of a glacier. The *specific balance B* is defined as the resultant of all processes in a year that lead to mass gain or loss at the surface on a unit area. The *cumulative balance* B_{cum} is the amount of mass gained or lost since the beginning of the 'balance year', normally taken at the end of the melt season. Winter balance and summer balance are other concepts used in glaciology. They are associated with the practice of measuring the cumulative balance twice a year: at the end of the winter and at the end of the summer. Various units are used for specific balance: m of water equivalent and $kg.m^{-2}$ are most common now.
In all glaciers and ice sheets the movement is from higher to lower parts. Ice flows from the *accumulation region*, where the annual mass balance at the surface is positive, to the *ablation region*, where the balance is negative. Those regions are separated by the equilibrium line (figure 1.1). The equilibrium-line altitude h_E is often used as a first basic parameter to describe the climatic conditions.
Various processes contributing to accumulation can be identified. Snowfall is most common, and a pack of snow gradually densifies to form firn (old snow that survived a summer) and, after several years, glacier ice. In the accumulation region melting may occur in summer, of course. However, in most cases the melt water does not run-off, but penetrates into the snow. Refreezing then warms the snow/firn layer through release of latent heat. Sometimes superimposed ice is formed. This occurs at places with a large seasonal cycle (i.e. at higher latitudes). Melt water may refreeze on bare ice, and the vertical structure of the ice layers may become very complex (and useless for some purposes like obtaining specific records from an ice core). In contrast, in the very cold climate of central Antarctica accumulation is mainly by the steady sinking of tiny ice crystals, and there is never any melting.

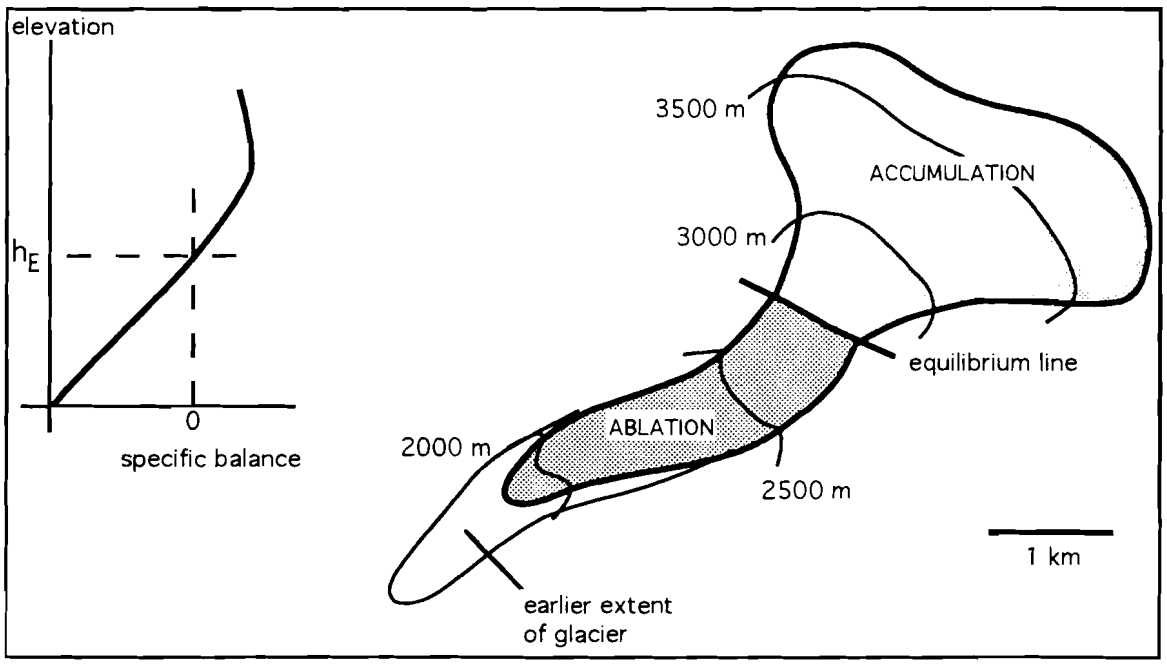

Figure 1.1. Typical geometry of a mountain glacier. The accumulation and ablation regions are seperated by the equilibrium line. A typical balance profile is shown at the left.

In the ablation zone a glacier looses its mass. It is general practice to compare the contributions from radiation and from the turbulent energy flux in the melting process. On most glaciers radiation is dominating, but the turbulent heat flux may play an important role in more maritime climates, in particular at the end of the summer, when solar radiation is less intense and warm air masses are advected from the sea.
For a glacier to be in equilibrium, conservation of mass requires that the following condition is met:

$$\int_{A_T} B \, da + C = 0 \qquad (1.1)$$

Here a is area, A_T the total area of the glacier, and C denotes the ice calving rate (≤ 0) in the case that calving in a lake or sea occurs. Since the rate of ablation can be much faster than the rate of accumulation, it follows from eq. (1.1) that the accumulation zone is generally much larger than the ablation zone.
On the Antarctic Ice Sheet ablation is negligibly small and the balance is essentially between accumulation and calving. On the Greenland Ice Sheet, ablation and calving are roughly of equal importance. The difference in the mass balance characteristics of these ice sheets are due to differences in temperature. The Antarctic continent is 20 to 30 K colder than Greenland.

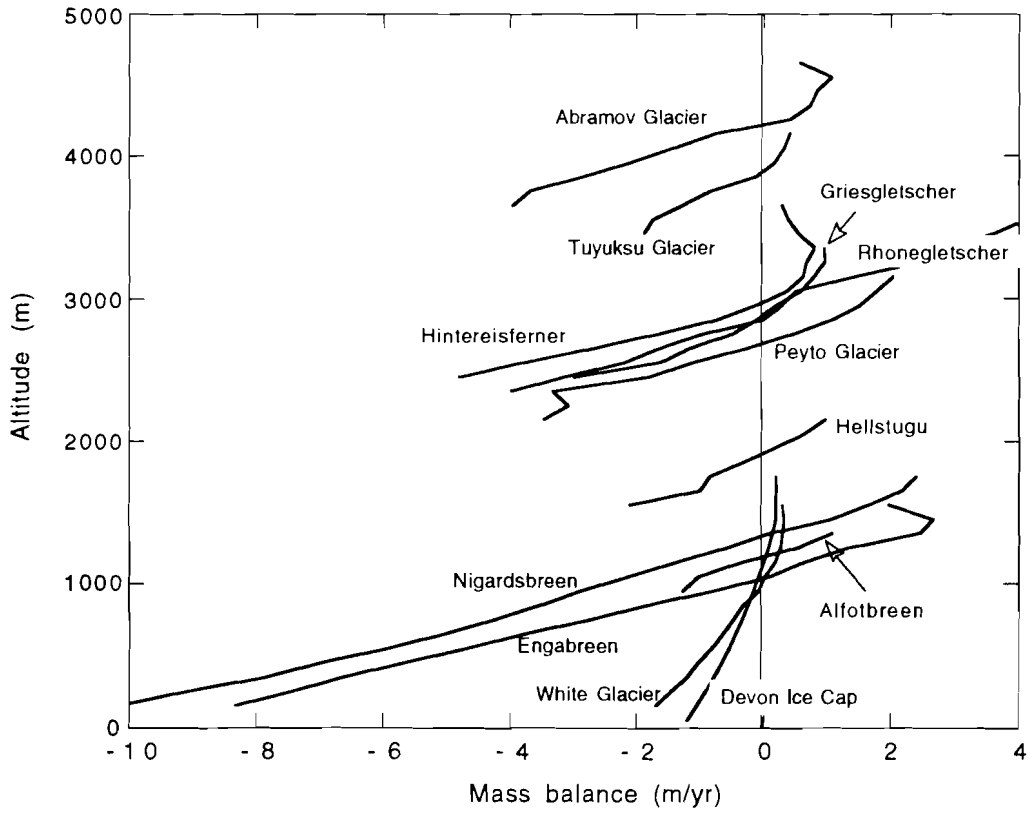

Figure 1.2. Measured balance profiles for glaciers in different climates. Note the large differences in balance gradients and maximum accumulation. From Oerlemans and Fourtuin (1992). Based on Kasser (1967, 1973), Müller (1977), Haeberli (1985) and Haeberli and Müller (1988), with additions.

On mountain glaciers, the specific balance depends first of all on elevation. This makes the concept of the balance profile useful. The *balance profile* $B(h)$ is defined as the specific balance in dependence of elevation h, where the value of B for a particular elevation is understood to be averaged over all points on a glacier having that elevation. In effect, this means that the mass balance is averaged along isohypses on the glacier, which run more or less perpendicular to the general flow direction.
In all practical applications elevation intervals are used. The condition of equilibrium can then be written as:

$$\frac{1}{A_T} \sum_i B(h_i)\, A(h_i) + C = 0 \qquad (1.2)$$

The index i refers to the elevation interval centered around h_i. In most mass balance studies the elevation interval is taken as 50 or 100 m. Mass balance profiles for 12 glaciers for which good measurements exist are shown in figure 1.2. Glaciers in the drier polar and subpolar regions, like Devon ice cap and White glacier in the Canadian arctic, have small balance gradients. Engabreen and Nigardsbreen, situated in Norway, have a tremendous mass turnover and large balance gradients. This also applies to the Rhone glacier in the Swiss Alps. The mass turnover of Hintereisferner (Austrian Alps) is somewhat less. Hellstugubreen is located in the drier part of southern Norway and Peyto glacier in the central Rocky Mountains in Canada. Abramov glacier and Tuyuksu glacier are in central Asia.

Ice flows from the accumulation zone to the ablation zone. The body force making the ice move is proportional to the surface slope s and the ice thickness H. As accelerations are negligibly small, this force must balance internal friction and the drag at the glacier bed (and to some extent at the sides). A typical velocity profile is shown in figure 1.3. It has two components: slip and deformational velocity. A the bed the ice velocity is the slip or sliding velocity u_s. The deformational component $u_d(z)$, where z is height above the bed, increases from zero to a maximum value at the glacier surface.

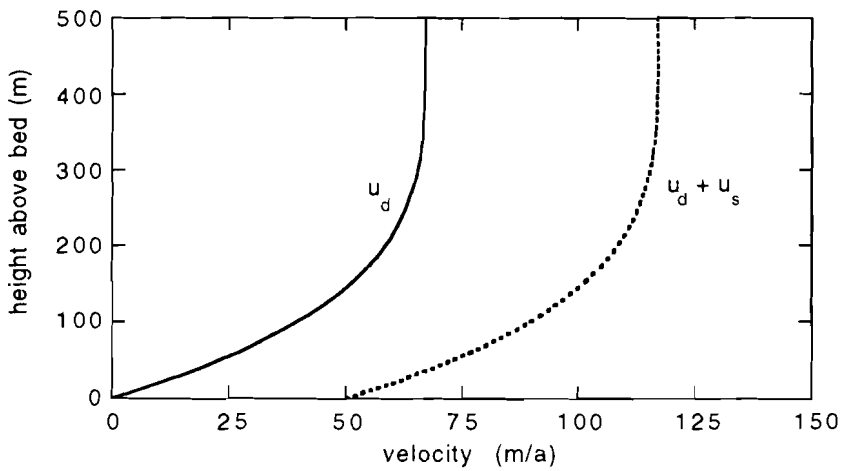

Figure 1.3. Example of a theoretical velocity profile for simple glacier flow. Solid line: deformation only. Dashed line: including a sliding velocity of 50 m/a.

The deformation of (fictive) parallel ice layers induces shear stresses at the interface of the layers. This shear stress must increase with depth, as it has to hold more and more ice in balance (the whole column of ice on which the body force is working). In a material like ice, a larger shear stress implies a larger velocity gradient, so $|du_d/dz|$ increases with depth too. A derivation of the velocity profile under certain simplifying assumptions will be given in a later section.

Historical data on glacier fluctuations concentrate on positions of glacier fronts, as this is the most easily observable quantity. Some information goes back to the late 16th century (Untere Grindelwaldgletscher). Data on glacier thickness / volume are much more scarce - some information is available for a few European glaciers (last 100 years).
The response of the position of a glacier front to climate change is the outcome of a process that has several steps. Modelling this response requires an approach in which the two main modules are compatible. A general scheme is shown in figure 1.4. The *mass-balance model* (MB-model) should translate changes in meteorological conditions into changes in specific balance. This serves as forcing for the *ice flow model* (IF-model), which delivers changes in glacier geometry in the course of time.

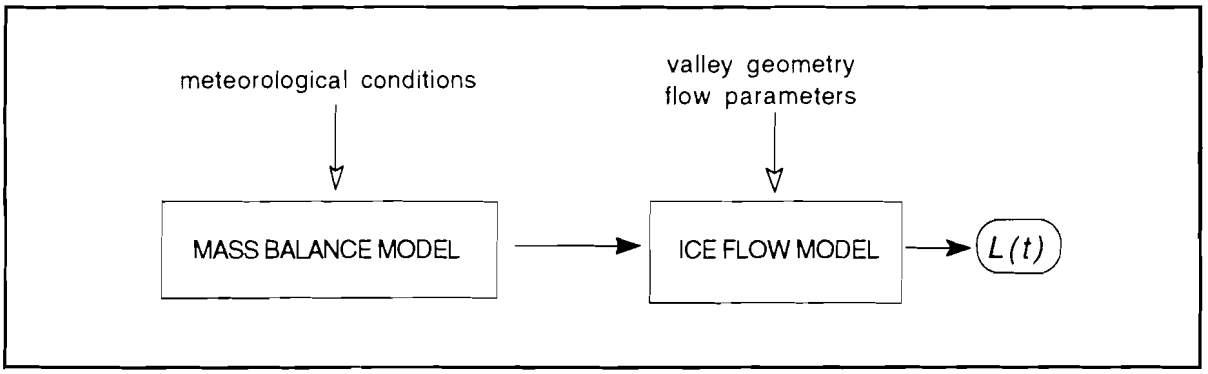

Figure 1.4. The simulation of changes in glacier length L requires coupling of a mass balance model, calculating from meteorological input data the specific balance as a function of elevation, to an dynamic ice flow model.

2. Historic glacier fluctuations - records > 200 years

Six well-known long records are shown in figure 2.1. In all cases the curves give glacier length, in the case of Vatnajökull the mean of 5 outlet glaciers from the ice cap (implying some smoothing). Glacier d' Argentière is in the French Alps, the Rhonegletscher and the Untere Grindelwaldgletscher in Switzerland, the Hintereisferner in Austria, Nigardsbreen in southern Norway and Vatnajökull in Iceland. The reliability of the records is probably relatively good (relatively = compared to other proxy indicators from historical documents like harvest data, dates of early/late frost, length of growing season, etc.). Details are subject to uncertainty, but this applies much less to the long-term variations.

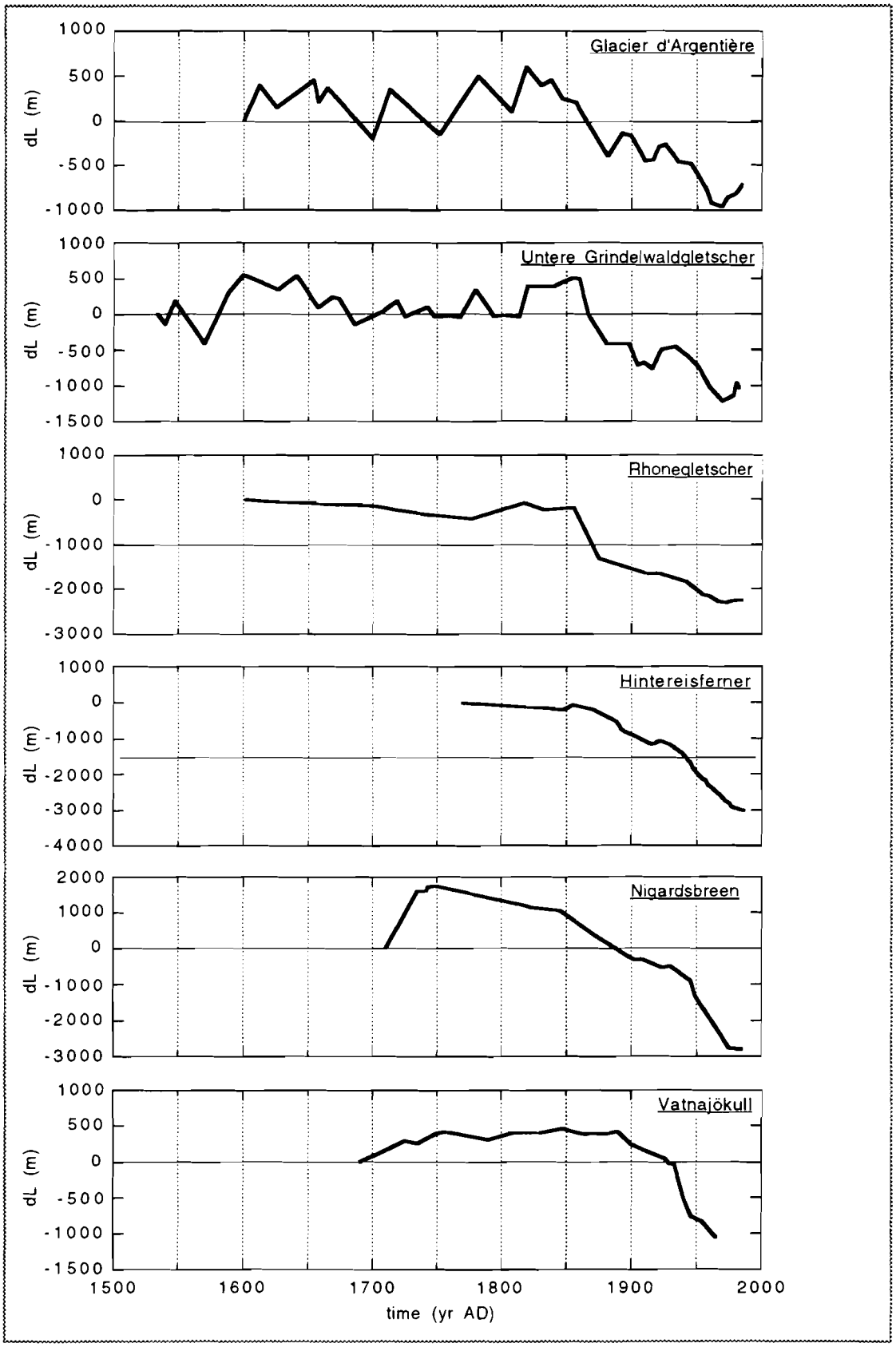

Figure 2.1. Six long records of historic variations of glacier length. For data sources, see Oerlemans (1988).

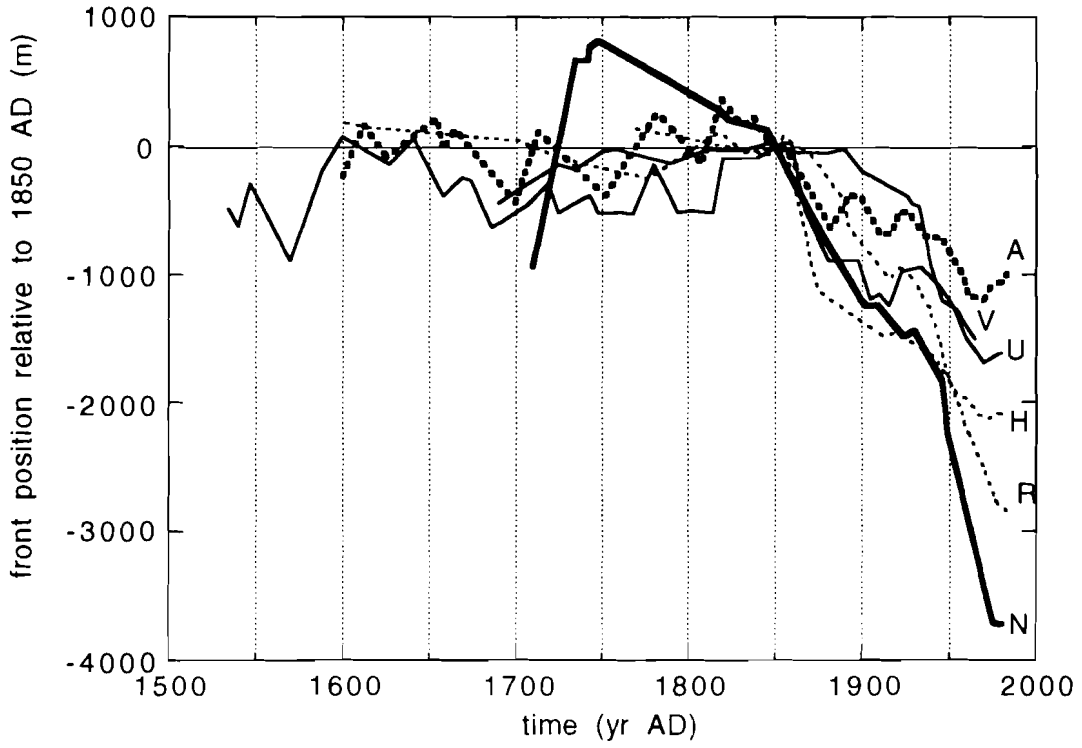

Figure 2.2. The same records as in figure 2.1, but now front position relative to 1850 AD, which marks the beginning of world-wide glacier retreat. Nigardsbreen shows the largest amplitude, Glacier d' Argentière the smallest. Characters refer to the various glaciers in figure 2.1.

The records are mainly based on:
- drawings and paintings
- descriptions in historical documents
- dating of end moraines
- measurements of distance of glacier front to benchmarkes (in more recent time)

In figure 2.2 these records are plotted together, and in all cases 1850 AD was taken as a reference point. Nigardsbreen has shown the largest retreat, it is also the largest glacier of this set.

Attempts have been made to model the historic fluctuations of Nigardsbreen (Oerlemans, 1986), Glacier d' Argentière (Huybrechts, 1989), Rhonegletscher (Stroeven and Van de Wal, 1989) and Hintereisferner (Greuell, 1992). In these studies climatological series from nearby stations were used as input. Results were not very good, in general. The strong retreat during the last 100 years was only partly simulated. A general conclusion from these studies was that the glacier models used are adequate, but that the forcing has poor quality because (i) the climate series are not very reliable, and (ii) the local aspects of the relation between climate and mass balance are not very well understood.

3. Why are glaciers sensitive to climate change ?

Climate sensitivity is a relative notion. Some quantities, like sea-ice extent, snow cover or water balance, have been claimed to react particularly strong to changes in climate. Concerning mountain glaciers, a number of interesting points can be made. Whether glaciers are more sensitive than other elements in some *absolute sense* is open to debate. Here we discuss the following aspects:

- the elevation - mass balance feedback
- melting rates and perturbed radiation balance

3.1 The elevation - mass balance feedback

The most powerful feedback mechanism associated with the growth and decay of ice sheets and glaciers is the feedback of increasing surface elevation on the specific balance. As clearly illustrated by figure 3.1, higher elevation generally implies larger balance. In fact, the glacial cycles of the Pleistocene would not have been possible without the elevation - mass balance feedback (Weertman, 1961; Oerlemans, 1980, 1981; Hyde and Peltier, 1986). The strength of the feedback depends on the balance gradient, of course, but also on the rate at which glacier thickness increases with glacier size. This rate is larger when the bed slope is smaller, so glaciers on a slightly inclined bed should be more sensitive to climate change than glaciers on a steep bed. This issue can be investigated with a very simple model.

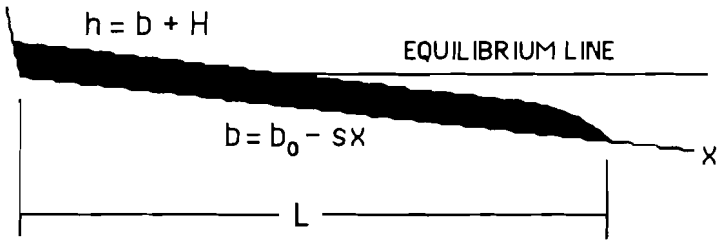

Figure 3.1. A glacier on a bed of constant slope *s*. Elevation of bed is *b*, of the ice surface *h*. *L* is the length of the glacier.

We consider a valley glacier on a bed with constant slope, see figure 3.1. We assume that the specific balance is a linear function of height relative to the equilibrium-line altitude h_E , i.e. $B = a\,(h-h_E)$. So a now is the balance gradient. According to eq. (1.1), the glacier is in equilibrium when

$$\int_L B\,dx = a\int_L (H+b_0-sx-h_E)\,dx = 0 \qquad (3.1)$$

This equation is easily integrated and solved for L:

$$L = \frac{2\,(H_m + b_0 - h_E)}{s} \qquad (3.2)$$

Here H_m is the mean ice thickness. It is noteworthy that in this case the solution does not depend on the balance gradient. Next the assumption is used that mean ice thickness times mean surface slope is constant (this is exactly true if ice would deform as a perfectly plastic material). So, in a first approximation:

$$H_m\, s = \frac{\tau_y}{\rho\, g} \qquad (3.3)$$

Here ρ is ice density, g acceleration of gravity and τ_y the yield stress. A typical value for the yield stress is 10^5 Pa (1 bar). As a characteristic value for the right hand side we thus use 11 m. Combining eqs. (3.2) and (3.3) yields:

$$L = \frac{2}{s}\left(\frac{\tau_y}{\rho\, g\, s} + b_0 - h_E\right) \tag{3.4}$$

Several conclusion can be drawn from this. First of all, for given b_o and h_E, a glacier will be much longer when the slope of the bed is small. Secondly, the ice thickness - mass balance feedback, reflected by the first term in the brackets, is more significant when the bed slope is smaller. We can define the climate sensitivity for this (extremely simple) glacier model as:

$$\frac{dL}{dh_E} = \frac{2}{s} \tag{3.5}$$

The results of this analysis are illustrated in figure 3.2. In the range of bed slopes where large mountain glaciers are normally found (0.1 to 0.2) the difference between L[variable thickness] and L[constant thickness] is large: for a 0.1 bed slope glacier length would be halved if glacier thickness would not affect the specific balance. In this calculation constant thickness is the thickness for a 0.4 slope (which is, for the values of the yield stress chosen earlier, 27.5 m). The other graph in figure 3.2 shows the climate sensitivity $2/s$. A typical value for large mountain glaciers is 15, implying that a 100 m drop in equilibrium-line altitude would make a glacier 1.5 km longer. This is typically the order-of-magnitude of the glacier fluctuations seen in figure 2.1.

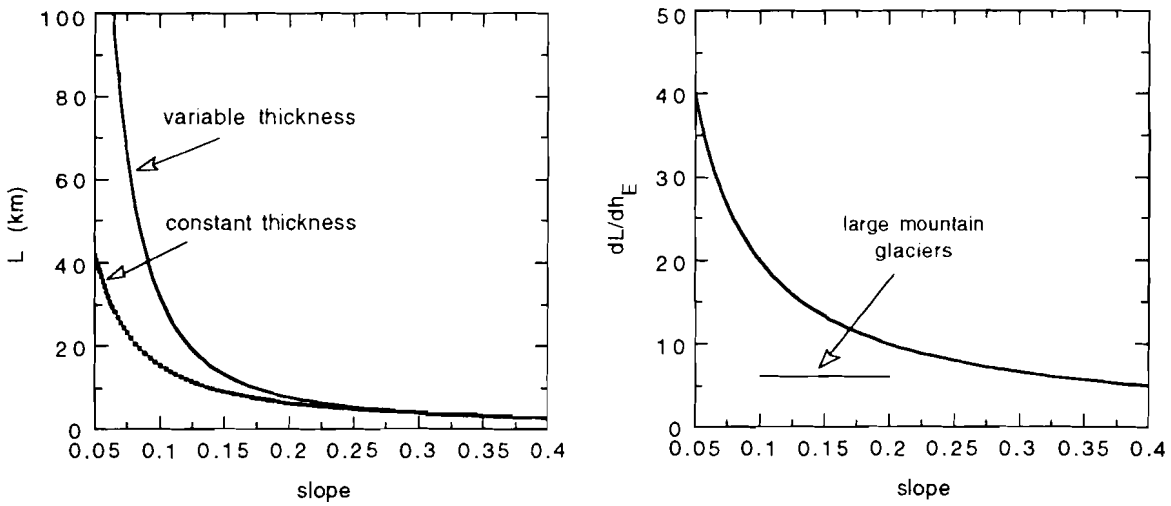

Figure 3.2. Dependence of ice thickness on mean bed slope (left). Curve labelled 'variable thickness' takes into account elevation - mass balance feedback. Picture at right shows sensitivity of glacier length to a change in equilibrium-line altitude. Parameter values: b_O= 3400 m, h_E = 2900 m.

How mean bed slopes actually vary is shown for the Alps in figure 3.3. This picture is based on World Glacier Inventory data for the Alps (Haeberli et al.,1989).

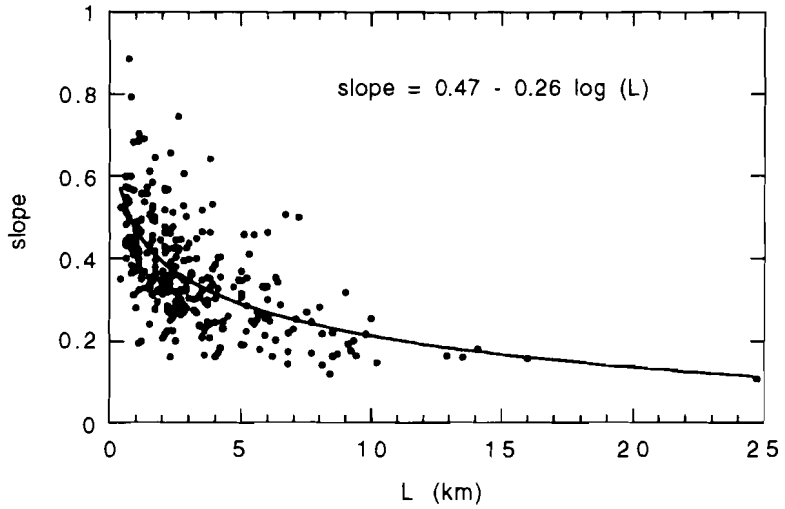

Figure 3.3. Estimated mean bed slope in dependence of length for glaciers in the Alps. Based on data for 298 glaciers.

The elevation - mass balance feedback leads to more complicated behaviour if the bed topography is irregular. In particular, as has been shown by numerical modelling, an *overdeepened bed* (bed slopes upward for some distance when going downglacier) creates bifurcation of the equilibrium states (Oerlemans, 1989). Also, varying glacier width, leading to thickening/thinning because of mass convergence/ divergence, plays an important role.

3.2 Melting rates and perturbed radiation balance.

The temperature of a melting glacier surface is fixed. This has an interesting consequence for the effect of a perturbation of the radiation balance at the surface. The energy budget Ψ at a melting glacier surface can be written as:

$$\Psi = (1-\alpha)G + I_{in} + I_{out} + F_t \qquad (3.6)$$

Here G is global radiation, α albedo, I_{in} and I_{out} incoming and outgoing longwave radiation flux, and F_t turbulent energy flux (latent and sensible heat). The conductive heat flux into the glacier can be neglected. Using the Brunt equation (e.g. Sellers, 1969) for incoming longwave radiation and a linear coefficient for turbulent exchange (K), eq. (3.6) can be written as:

$$\Psi = (1-\alpha)G + \sigma T_a^4 (c + d\sqrt{e}) + \sigma T_m^4 + K(T_a - T_m) \qquad (3.7)$$

Mean air temperature is denoted by T_a, the melting point of ice by T_m, vapour pressure at screen height by e; c and d are constants in the Brunt equation (mean values: a=0.61 en b=0.05 $hPa^{-0.5}$).
We now assume that all quantities refer to mean values over a typical fair weather day in summer. Outgoing longwave radiation is 316 $W.m^{-2}$, and this is also a typical value for absorbed solar radiation (at midlatitudes). So we suppose for convenience that these components, that do *not directly depend on air temperature*, cancel. The other terms are shown in figure 3.4. The calculated rate of change of ablation with temperature is 0.0038 mwe/K. For an ablation season equivalent to 100 of these days, the increase in melting would thus be 0.38 m per

degree. This is a substantial value. As much more sophisticated models have shown, this value is even larger because an increase in temperature also makes the melt season *longer*.
From a physical point of view, the large sensitivity of glacier mass balance to a change in air temperature stems from the fact that the surface temperature cannot increase, and therefore the *outgoing longwave radiation does not increase* (as is the case for a 'normal' soil). The situation is somewhat comparable to the tropics, where additional energy is used for evaporation rather than increasing the surface temperature (and, consequently, the rate of evaporation is a better climate indicator here than air temperature, but more difficult to measure).

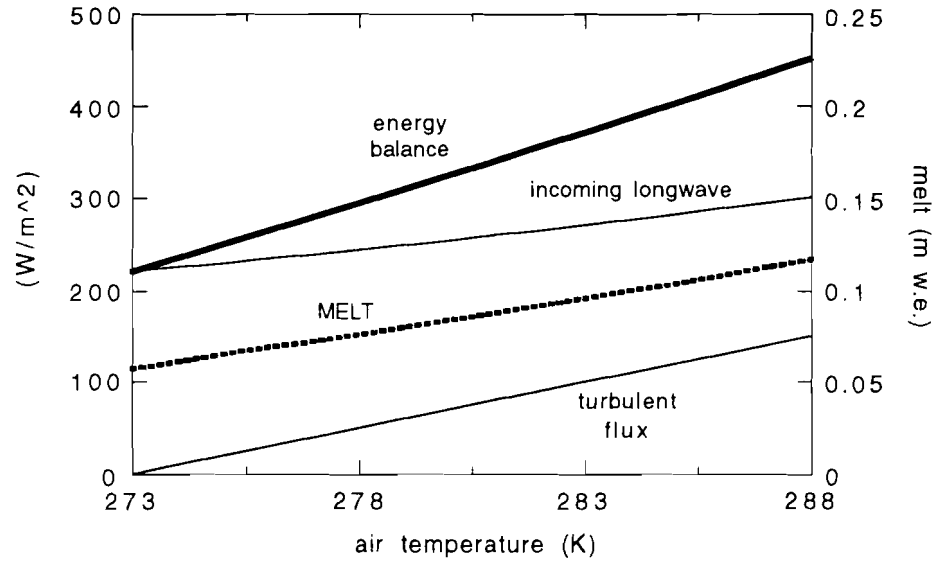

Figure 3.4. Energy balance of a melting glacier surface in dependence of air temperature. Outgoing longwave and absorbed shortwave radiation are not shown (both equal 316 $W.m^{-2}$). Relative humidity is 75%.

4. Modelling the evolution of valley glaciers - glacier flow

In this chapter models are described that can be used for the study and simulation of historic glacier fluctuations. As explained in the introduction, two modules are needed: one relating climate to glacier mass balance, and one describing glacier flow as response to imposed mass balance. First glacier flow will be considered.

4.1 Plane shear flow

Simple shearing flow is discussed, implying that longitudinal stress gradients have little effect on the ice motion. For glaciers this is a reasonable assumption as long as length scales of several times the ice thickness are considered (e.g. Paterson, 1981). In this case, the motion is entirely determined by one component of the stress tensor namely τ_{xz}. Here z is the vertical coordinate, x is the horizontal coordinate in the direction of the flow. The shear stress is given by

$$\tau_{xz} = \rho g(H-z)\, s \qquad (4.1)$$

Here ρ is ice density, g acceleration of gravity, s (=dh/dx, where h is surface elkevation) surface slope and H ice thickness. For a Glen-type flow law, with exponent 3, the following expression for the velocity gradient then holds:

$$\frac{du}{dz} = 2A\left\{\rho g(H-z)\, s\right\}^3 \tag{4.2}$$

Ice viscosity is denoted by A. It depends on cristal size and fabric, concentration and type of impurities, and ice temperature. As here the interest is mainly in temperate glaciers, A is assumed to be constant. Eq. (4.2) can then be integrated from the bed upwards to give:

$$u(z) = U_s + \frac{A}{2}(\rho g s)^3\left\{H^4 - (H-z)^4\right\} \tag{4.3}$$

U_s is the sliding velocity. One more integration yields the vertical mean velocity:

$$U = U_s + \frac{A}{10} H \tau_b^3 = U_s + U_d \tag{4.4}$$

So the mean velocity due to deformation is directly related to the base stress τ_b (also termed 'driving stress' in this context). Eq. (4.3) shows that the deformational ice velocity increases very strongly with driving stress. This reflects the nonlinear character of ice deformation: little deformation when forces are small, very large deformation when forces are large. As a result, ice flows in such a way that a tendency towards constant base stress exists, i.e. sH = constant (this assumption was used in section 3.1).

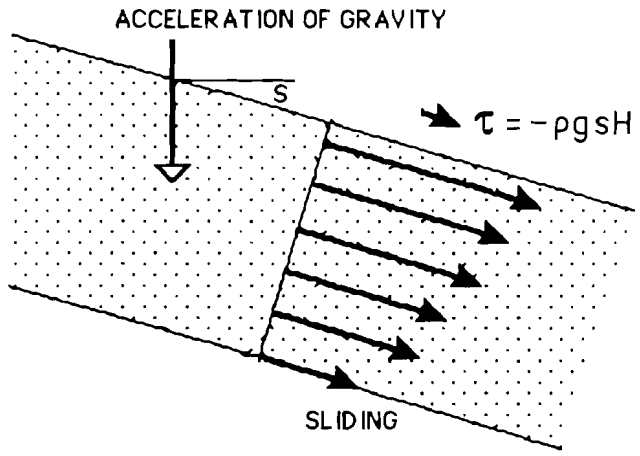

Figure 4.1. Both sliding and deformation contribute to the mass flux. The driving stress τ increases linearly with surface slope s and ice thickness H.

A frequenly used expression for glacier flow, based on eq. (4.4) and extended to include a parameterization of sliding, reads:

$$U = U_d + U_s = f_d H \tau^3 + \frac{f_s \tau^3}{P} \tag{4.5}$$

The subscripts *d* and *s* refer to deformation and sliding, respectively. The parameter f_d now is a generalized viscosity. The sliding is supposed to be proportional to the third power of the base stress as well, but divided by the water pressure at the bed (P). Attempts have been made to obtain a theoretical expression for the sliding parameter f_s, but a concensus has not yet been reached. Both f_d and f_s should be considered as semi-empirical parameters, varying from glacier to glacier.

4.2 Change in ice thickness

If the vertical mean velocity vector is denoted by **U**, the volume flux of ice is given by $H\,\mathbf{U}$. Ignoring differences in ice density, the local rate of change of ice thickness can be obtained by vertically integrating the continuity equation for an incompressible fluid. This yields (e.g. Oerlemans and Van der Veen, 1984):

$$\frac{\partial H}{\partial t} = -\nabla.(\mathbf{U}H) + B \qquad (4.6)$$

This equation forms the basis for many numerical studies of the the dynamics of glaciers and ice sheets. It is frequently used in one-dimensional form in *flow-line models*, where the dynamics of a glacier are calculated along a central line down the surface slope (but still taking into account varying lateral geometry). This is illustrated in figure 4.2.

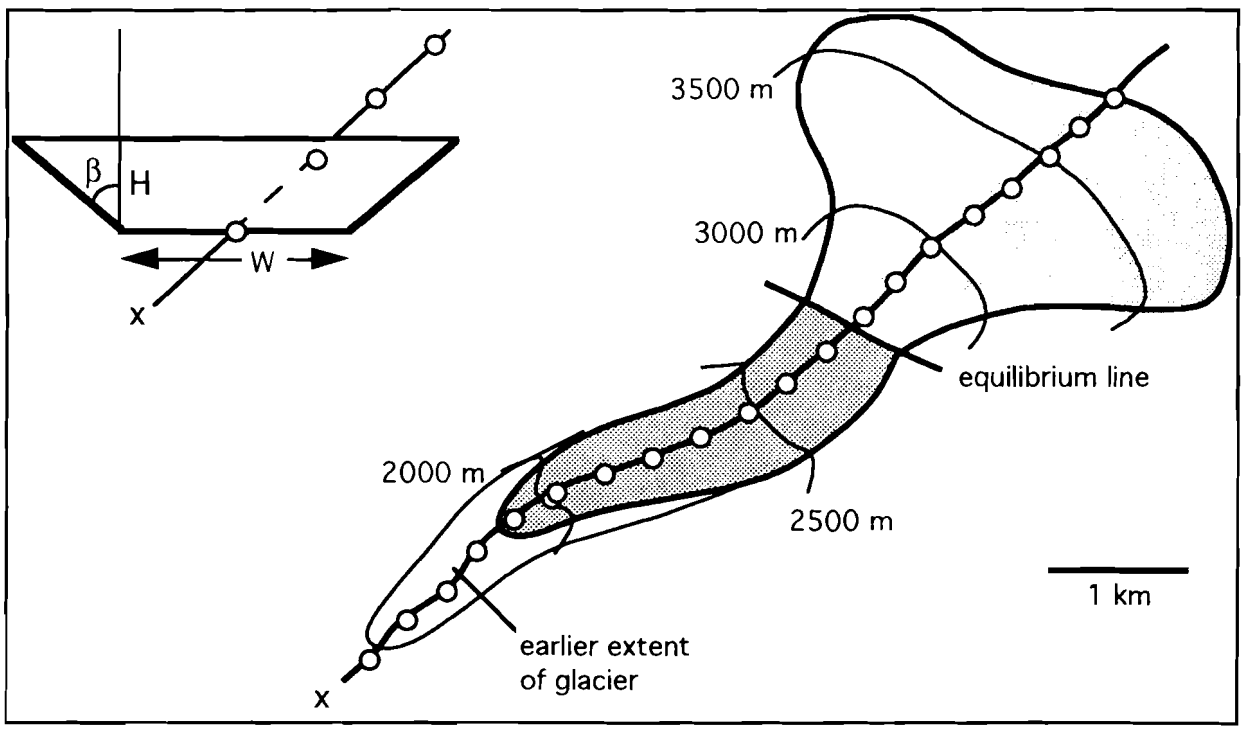

Figure 4.2. Constructing a numerical flow model for a mountain glacier. Grid points are equidistant along the horizontal coordinate *x*. The *x*-axis follows the course of the valley.

If S is the area of the cross section of a glacier perpendicular to the flow line, mass conservation can be expressed as

$$\frac{\partial S}{\partial t} = -\frac{\partial (US)}{\partial x} + BW_s \tag{4.7}$$

Here W_S is the glacier width at the surface. To relate S to ice thickness, a shape for the cross section has to be assumed. With a trapezoidal shape it follows that:

$$S = H\{B + H\,tg(\beta)\} = H(B + mH) \tag{4.8}$$

It is easily verified that the rate equation for H becomes

$$\frac{\partial H}{\partial t} = \frac{-1}{B + 2\mu H}\frac{\partial}{\partial x}\left[(B + \mu H)UH\right] + B \tag{4.9}$$

The mass balance is normally specified as a function of h. So

$$B = B(h), \quad with \;\; h = b(x) + H(x,t) \tag{4.10}$$

Here b is the bed elevation. With the set of equations [(4.5), (4.9) and (4.10)] the evolution of the glacier can be calculated.

5. Modelling the evolution of valley glaciers - mass balance

5.1 The energy balance

The energy balance equation at the surface forms the basis for the calculation of the mass balance. The temperature profile in the upper layers of the glacier is not calculated, but an arrangement is made to deal with refreezing in spring / early summer.
The basic equations read:

$$\Psi = (1-\alpha)G + I_{in} + I_{out} + H_s + H_l \tag{5.1}$$

$$B = \int_{year} \left\{(1-f)\,min\,(0;-\Psi/L) + P^*\right\} dt \tag{5.2}$$

In eq. (5.1), the energy balance consists of absorbed solar radiation (α is albedo, G global radiation), incoming and outgoing longwave fluxes (I_{in} and I_{out}), and the turbulent fluxes of sensible and latent heat (H_s and H_l). It is assumed that melting occurs at the surface as soon as the energy balance becomes positive. L is the latent heat of melting. In eq. (5.2), f is the fraction of the melt water that refreezes and does not contribute to mass loss. P^* is set to zero when air temperature is above 2°C, and equal to the precipitation rate otherwise. Eq. (5.2) is integrated using one day as time step (in contrast to some earlier work, e.g. Oerlemans (1992), where the daily cycle was calculated explicitly).
Meltwater that penetrates into the snowpack with a temperature below the melting point will refreeze and not run off. This process is dealt with by specifying that the

fraction of melt energy involved in runoff, denoted by R, increases when the snow/ice temperature approaches the melting point. The equations used are:

$$R = \Psi \exp(c\, T_{ice}) \tag{5.3}$$

$$H_{ice} = \Psi - R = \Psi(1 - \exp(c\, T_{ice})) \tag{5.4}$$

$$C \frac{dT_{ice}}{dt} = H_{ice} \quad (T_{ice} \leq 0) \tag{5.5}$$

Here H_{ice} is the heat flux into the upper ice/snow layer. This layer is assumed to have a heat capacity equivalent to 2 m of solid ice (with a density of 900 kg/m3); its mean temperature is denoted by T_{ice} (in °C). The constant c determines how fast the fraction of melted snow that runs off approaches one. Here c was set to one.
When the integration is started, normally at day 300, the ice temperature is set equal to the annual mean air temperature. This temperature can then only be changed by refreezing melt water in the beginning of the ablation season. So at higher elevations, where temperatures are lower, more snow has to be melted before the cold layer is heated up and significant runoff may start. The layer thickness of 2 m is rather ambiguous, but, concerning the amounts of energy involved, in line with the findings of Ambach (1963).
There are several reasons why the integration has to be extended over 2 or 3 years. First, the initial conditions cause transient effects which take over a year to die out. This applies in particular to the albedo ($a = a_b$ at $t = 0$). Second, the background albedo profile is tied to the height of the equilibrium line E, which can only be computed after a one year's integration; thus at least a second year has to be simulated. In practice it appears that the solution is in equilibrium after 3 yr , and in most cases after 2 yr (i.e. after one iteration). Care has to be taken concerning initial conditions: mass balance, accumulated melt, snow depth and ice temperature are initialized again every year, but albedo and equilibrium-line altitude not.

5.2 Radiation

In the calculation of the global radiation reflecting slopes and shading effects are ignored. The equation for atmospheric transmissivity for solar radiation reads:

$$t_{atm} = \{0.79 + 2.4 \cdot 10^{-5}\, h\}\{1 - (0.41 - 6.5 \cdot 10^{-5}\, h)\, n - 0.37\, n^2\} \tag{5.6}$$

Cloudiness is indicated by n (running from 0 to 1). Daily mean values of insolation on a horizontal plane of unit area at the top of the atmosphere are required as input. These are multiplied by t_{atm} to obtain global radiation at the surface. The approximation for the effect of clouds on atmospheric transmissivity fits the experimental results of Sauberer (1955).
Performance of an energy balance model in simulating glacier mass balance depends to a large extent on the way albedo is treated. Albedo varies strongly in space and time, depending on the melt and accumulation history itself. There are significant feedbacks involved, implying that a mass balance model designed to study the response to climate change must generate the albedo internally. This is difficult, however, as so many factors are involved. The albedo depends in a complicated way on crystal structure, ice and snow morphology, dust and soot concentrations, morainic material, liquid water in veins, water running across the

surface, solar elevation, cloudiness, etc. The best one can do is to construct a simple scheme, in which the gross features broadly match available data from valley glaciers.
Accumulation of atmospheric dust and morainic material clearly is a very important factor. It is reasonable to assume that *the concentrations found at the surface depend on the location relative to the equilibrium line*, as this determines the annual mean vertical ice velocity at the surface. So, as starting point a 'background albedo profile' is defined:

$$\alpha_b = 0.43 + \frac{0.18}{p} \operatorname{arctg}\left(\frac{h - h_E + 300}{200}\right) \qquad (5.7)$$

Here h and E are in m. The constants appearing in eq. (5.7) have been found after much experimentation as giving good results (in terms of the simulation of the typical albedo pattern on a valley glacier at the end of the ablation season). The α_b-profile is shown in figure 5.1.

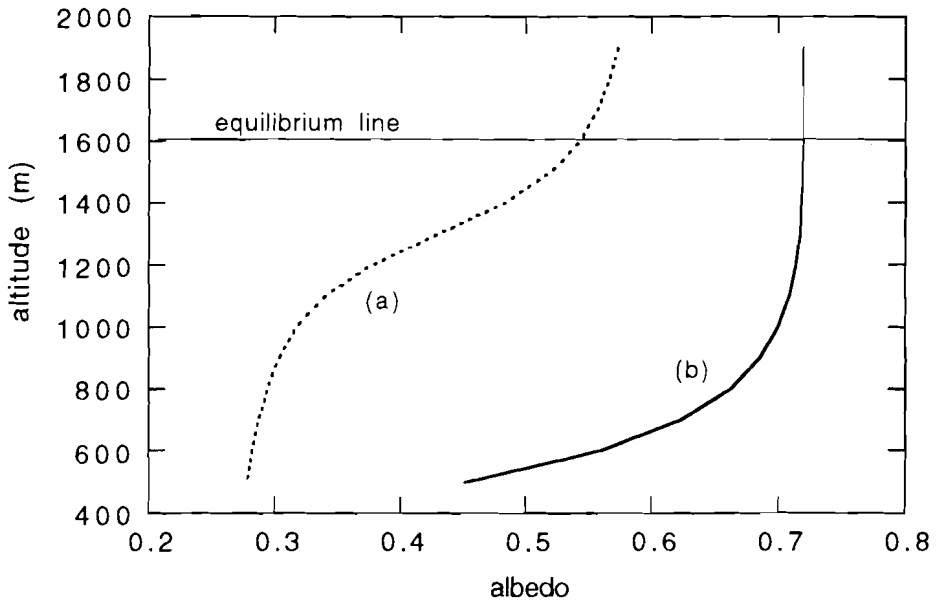

Figure 5.1. Background albedo profile as formulated in eq. (5.4). The equilibrium-line altitude is set to 1600 m. The effect of an additional snow cover, increasing linearly from 0.1 m at 500 m elevation to 1.5 m (water equivalent) at 1900 m elevation is illustrated by curve (b).

As snow on the lower parts of glaciers normally occurs in patches, it is realistic to make the increase of albedo a smooth function of snow depth d (in m water equivalent), in such a way that a smooth transition between α_b and the snow albedo is obtained. The expression used for α reads:

$$\alpha = \alpha_{sn} - (\alpha_{sn} - \alpha_b)\, e^{-5d} \qquad (5.8)$$

Here, snow albedo α_{sn} is assumed independent of the age of the snow. The justification for this assumption is that the modelling of precipitation is too schematic for a detailed treatment of age-effects. To compensate for this simplification, the snow is assumed to have a standard age, and the value for a_{sn} is suitably reduced below that for fresh snow, namely 0.72.

The calculation of incoming longwave radiation follows an approach similar to Kimball et al. (1982). Two contributions are distinguished: one from the clear-sky atmosphere (but originating from the lowest tens of meters of the atmosphere), and one (denoted by I_{cl}) originating at the base of clouds and transmitted in the 8 - 14 μm band (atmospheric window), i.e.

$$I_{in} = \varepsilon_a \sigma T^4 + I_{cl} \tag{5.9}$$

The atmospheric emissivity is written in terms of water vapour pressure e_a (in Pa) and air temperature T (in K, 2 m above the surface):

$$\varepsilon_a = 0.7 + 5.95 \times 10^{-7}\, e_a\, e^{(1500/T)} - 2.5 \times 10^{-5}\, h \tag{5.10}$$

The decrease of atmospheric emissivity with altitude thus obtained (i.e. because vapour pressure and temperature normally decrease with alitude) appears to be somewhat less than generally observed (Müller, 1984). The last term in eq. (5.7) deals with this. The cloud contribution to the long wave radiation balance is written as:

$$I_{cl} = n\, f\, \sigma\, T_{cl}^4 \tag{5.11}$$

Temperature of the cloud base is denoted by T_{cl}. The factor f is the product of cloud base emissivity, mean fraction of radiation emitted in the atmospheric window, and transmissivity of air between surface and cloud base in the window. Here f was set to a value of 0.25. I_{out} is simply taken as the radiation emitted by a block body at the melting point, i.e. 315.6 W/m^2. This value will overestimate the long-wave balance if the skin temperature is below the freezing point. However, as the energy balance is only relevant when melting occurs, the assumption of zero surface temperature will only lead to a small error in the simulated mass balance (see also the discussion in Greuell and Oerlemans, 1987).

5.3 Turbulent fluxes

Turbulent fluxes over melting ice/snow surfaces can be quite large in spite of the stable atmospheric statification normally encountered. Compared to other atmospheric boundary layers, much of the turbulent kinetic energy is concentrated in relatively small scales, and thus existing theory for stable boundary layers may underestimate the turbulent fluxes. As, over ice, for most cases surface roughness and climatological wind conditions are unknown, a constant exchange coefficient C is used in the hope that the bulk effect of the fluxes is captured. The equations read:

$$H_s = C\,(T - T_s) \tag{5.12}$$

$$H_l = 0.622\, \frac{C\,L}{c_p}\, \frac{(e_a - e_{as})}{p} \tag{5.13}$$

Here T_s is surface temperature, c_p specific heat, p atmospheric pressure and e_{as} saruration vapour pressure over water [when the energy balance is positive] or ice [when the energy balance is negative]. The approximations used are (in Pa; see e.g. Kraus, 1972):

$$e_{as} = 610.8\, \exp\left\{19.85\left(1 - \frac{273.16}{T}\right)\right\} \quad \text{(over water)} \tag{5.14}$$

$$e_{as} = 610.8 \ \exp\left\{22.47\left(\frac{273.16}{T} - 1\right)\right\} \quad \text{(over ice)} \tag{5.15}$$

As the surface temperature is not calculated, T_s is replaced by the melting point. In Greuell and Oerlemans (1987), a comparison was made between a full calculation, in which temperature was actually resolved as a function of depth, and a calculation with surface temperature at the melting point all the time. The differences in accumulated melt appeared to be quite small.

5.4 Input data

Meteorological input data needed to run the model are temperature and humidity at standard measuring height, cloudiness, and precipitation. Air temperature T is generated by assuming sinusoidal shapes for seasonal variation:

$$T = M_T - \gamma_M h - A_T \cos\left[2\pi(N_{day} - N_{shift})/365\right] \tag{5.16}$$

M_T is annual mean temperature reduced to sea level, and γ_M lapse rate of annual mean temperature. N_{day} is the day number (1 January corresponds to $N_{day} = 1$) and N_{shift} the date of maximum temperature to be prescribed.
Daily mean values of insolation at the top of the atmosphere are also needed as input to the energy balance calculations.
The largest uncertainty generally concerns the altitudinal gradients of the input parameters, especially precipitation.

6. Coupling mass balance and flow model

The existing ice flow model uses an explicit scheme for time integration, implying that the time step has to be rather small (~ 0.2 yr). In principle it is possible to run the mass balance model and ice flow model simultaneously, but this is not very efficient. It is more practical to do the mass balance calculations on a grid uniform in altitude, and make a polynomial fit to the output, i.e. $B = b_1 + b_2\ h + b_1\ h^2$. Normally a second-order polynomal would do. This has the advantage that the mass balance model needs not to be rerun when the glacier geometry has changed only.
In case of climate forcing, the mass balance can be run every 5 or 10 years when desired.

References

Ambach W (1963): Untersuchungen zum Energieumsatz in der Ablationszone des Grönlandischen Inlandeises. *Meddelelser om Grønland* **174** (4), 311 pp.

Greuell W and J Oerlemans (1987): Sensitivity studies with a mass balance model including temperature profile calculations inside the glacier. *Zeits. Gletscherk. Glazialgeol.* **22**, 101-124.

Greuell W (1992): Hintereisferner, Austria: mass-balance reconstruction and numerical modelling of the historical length variations. *J. Glaciol.* **38**, 233-244.

Haeberli W (1985): *Fluctuations of Glaciers, 1975-1980.* (Vol. IV) IASH (ICSI)- UNESCO.

Haeberli W, H Bösch, K Scherler, G Østrem and C C Wallén (1989): *World Glacier Inventory. Status 1988.* IAHS(ICSI)-UEP-UNESCO.

Haeberli W and P Müller (1988): *Fluctuations of Glaciers, 1980-1985.* (Vol. V) IASH (ICSI)- UNESCO.

Huybrechts Ph, P de Nooze and H Decleir (1989): Numerical modelling of Glacier d'Argentière and its historic front variations. In: *Glacier Fluctuations and Climatic Change.* (ed.: J Oerlemans), Reidel, 373-389.

Hyde W T and W R Peltier (1985): Sensitivity experiments with a model of the ice-age cycle: the response to Milankovitch forcing. *J. Atmos. Sci.* **44**, 1351-1374.

Kasser P (1967): *Fluctuations of Glaciers, 1959-1965.* (Vol. I) IASH (ICSI)- UNESCO.

Kasser P (1973): *Fluctuations of Glaciers, 1965-1970.* (Vol. II) IASH (ICSI)- UNESCO.

Kraus E B (1972): *Atmosphere-Ocean Interaction.* Oxford University Press, 275 pp.

Müller F (1977) Fluctuations of Glaciers,1970-1975. (Vol. III) IASH (ICSI)- UNESCO.

Oerlemans J (1980): Model experiments on the 100 000 yr glacial cycle. *Nature* **287**, 430-432.

Oerlemans J (1981): Some basic experiments with a vertically-integrated ice-sheet model. *Tellus* **33**, 1-11.

Oerlemans J (1986): An attempt to simulate historic front variations of Nigardsbreen, Norway. *Theor. Appl. Climatol.* **37**, 126-135.

Oerlemans J (1988): Simulation of historic glacier variations with a simple climate-glacier model. *J. Glaciology* **34**, 333-341.

Oerlemans J (1989): On the response of valley glaciers to climatic change. In: *Glacier Fluctuations and Climatic Change.* (ed.: J Oerlemans), Reidel, 353-371.

Oerlemans J (1992) Climate sensitivity of glaciers in southern Norway: application of an energy-balance model to Nigardsbreen, Hellstugubreen and Alfotbreen. J Glaciology 38: 223-232.

Oerlemans J and J P F Fortuin (1992) Sensitivity of glaciers and small ice caps to greenhouse warming. *Science* **258**, 115-117.

Oerlemans J and C J van der Veen (1984): *Ice Sheets and Climate.* Reidel, 217 pp.

Paterson W S B (1981): *The Physics of Glaciers.* Pergamon Press, 2nd edition.

Sauberer, F (1955): Zur Abschätzung der Globalstrahlung in verschieden Höhenstufen der Ostalpen. *Wetter und Leben,* **7**, 22-29.

Sellers W D (1969): *Physical Climatology.* The University of Chicago Press (London), 272 pp.

Stroeven A, R van de Wal and J Oerlemans (1989): Historic front variations of the Rhone glacier: simulation with an ice flow model. In: *Glacier Fluctuations and Climatic Change.* (ed.: J Oerlemans), Reidel, 391-405.

Weertman J (1961): Stability of ice-age ice sheets. *J. Geophys. Res.* **66**, 3783-3792.